International Journal of Nanoelectronics and Materials
IJNeaM
ISSN 1985-5761 | E-ISSN 2232-1535

Pure and Doped Gallium Nitride-Based Gas Sensor: A Review

Sarmad Fawzi Hamza Alhasan[a], Mothana A. Hassan[b], Zaid T. Salim[c], Reem M. Khalaf[d], Makram A. Fakhri[b,*] , Motahher A. Qaeed[e], Ahmed A. Al-Amiery[f], Subash C. B. Gopinath[g,h,i]

[a]*College of Communication Engineering, University of Technology-Iraq, Baghdad, Iraq*
[b]*College of Laser and Optoelectronic Engineering, University of Technology-Iraq, Baghdad, Iraq*
[c]*College of Energy and Environmental Sciences, Al-Karkh University of Science, Baghdad 10081, Iraq*
[d]*Al-Farahidi University, Baghdad, Iraq*
[e]*Department of Physical Sciences, Faculty of Science, University of Jeddah, Jeddah, Saudi Arabia*
[f]*Al-Ayen Scientific Research Center, Al-Ayen Iraqi University, AUIQ, P.O. Box: 64004, An Nasiriyah, Thi Qar, Iraq*
[g]*Center for Global Health Research, Saveetha Medical College & Hospital Saveetha Institute of Medical and Technical Sciences (SIMATS), Thandalam, Chennai – 602 105, Tamil Nadu, India*
[h]*Faculty of Chemical Engineering & Technology and Institute of Nano Electronic Engineering, Universiti Malaysia Perlis (UniMAP), 02600 Arau, Perlis, Malaysia*
[j]*Department of Technical Sciences, Western Caspian University, Baku AZ 1075, Azerbaijan*
**Corresponding author. Tel.: +964y7702793869; e-mail: Makram.a.fakhri@uotechnology.edu.iq, mokaram_76@yahoo.com*

ABSTRACT

This paper shows how gallium-nitride-based gas sensors are frequently used for detecting toxic gases and vapors and gives an overview of how to use them with different layer thicknesses in order to detect multi-spectral ranges and to obtain high performance, high response, high speed, and low cost for gas sensor devices. The earlier published works are summarized, as is the gallium nitride material grown on different substrate materials such as silicon, sapphire, or quartz using different growth methods to fabricate sensors used in wide application fields such as environmental control, industrial monitoring, and household safety. GaN material-based gas sensors are considered to be promising to open a new generation of fields due to their virtues for designing high temperature, high frequency, and high power sensors.

Keywords: *Gas sensors, Electrochemical sensors, Doped Gallium nitride, Porous silicon, Doped GaN heterostructure*

1. INTRODUCTION

There's an important trend toward nanoscience and nanotechnology at present. Recent advances in nanoscience and technology are being driven by the fact that, as scales continue to shrink, new physical effects are becoming apparent that may be utilized in future technological applications [1, 2]. Due to the increased availability of nanomaterial synthesis techniques, their growth has exploded in the past decade. Moreover, as instruments for characterizing and manipulating nanostructures of semiconductors, metals, and other materials in order to gain a better understanding of them [3, 4], synthesis, exploration, characterization, and utilization of nanostructured materials are the focus of nanoscience and nanotechnology. These materials have at least one nanometer-scale dimension. The physical and chemical properties of nanomaterials differ from those of bulk materials and atomic-molecular materials of identical composition [5, 6]. Due to the nanometer size of the materials that render them, a significant fraction of surface atoms, high surface energy, spatial confinement, and reduced impurities do not exist in the bulk equivalents. Nanomaterials have a very high surface area-to-volume ratio due to their small size [7, 8]. Thin film science and technology serve a crucial role in high-tech industries. As two-dimensional systems, thin films are of considerable importance. The attractive properties of thin films differ from those of bulk materials. This is because their properties are dependent on a number of interconnected parameters as well as the fabrication technique [9, 10]. Nanostructures are commonly utilized as sensing layers for a variety of gas sensors. Using nanostructures as sensing layers provides large surface-to-volume ratios for gas molecule interaction, which has the potential to increase sensor sensitivity and response time in comparison to conventional thin film sensing layers. Moreover, their size, composition, and shape can be chemically modified to influence not only the sensors' sensitivity but also their selectivity [11, 12]. There is currently a great deal of interest in implementing sensing devices in order to enhance environmental and safety gas control. This type of sensor is also in high demand for optimizing combustion reactions in the emerging transportation industry and in domestic and industrial applications [13, 14]. Due to their potential applications in optoelectronic devices, the growth of GaN films and their properties have been intensively investigated over the past few years. Furthermore, in high-temperature and high-power electronic devices [15, 16], GaN can be used to create a variety of devices, including lasers, visible and ultraviolet LEDs, solar cells, and sensor materials. These substances can be heteroepitaxially grown on a variety of substrates. [17, 18]. There have been many reports of AlN, InN, GaN, and their compounds growing on substrates other than

sapphire, such as SiC, GaAs, and Si. The growth of GaN on Si substrates has been one of the most intriguing topics due to its large surface area, low cost, and excellent thermal and electrical conductivity. However, the growth of high-quality epitaxial GaN on Si substrates presents numerous challenges due to the large lattice mismatch and thermal expansion coefficient divergence between GaN and Si [19, 20].

2. GALLIUM NITRIDE PROPERTIES

III-nitride semiconductors are the preferred materials for numerous device applications. In the past few decades, gallium nitride (GaN) thin films have garnered the most academic and commercial interest among all III-nitrides [21, 22]. The direct energy band gap of III-nitride semiconductors is extensive. The band gap values for InN, GaN, and AlN are 0.7–1.9 eV, 3.4 eV, and 6.1 eV, respectively [23, 24]. The extensive spectrum of direct bandgaps corresponding to blue and ultraviolet ray emissions makes it suitable for optoelectronic devices [25, 26], including light-emitting diodes (LEDs), photodetectors, and laser diodes [27, 28]. Likewise, it is appropriate for high-power electrical instruments [29, 30]. In general, semiconductors composed of III-nitrides can be crystallized into both wurtzite and zinc-blende polyvarieties. However, the former is examined more extensively because it is thermodynamically more stable. III-nitride semiconductors have also been utilized for applications involving high temperatures and high frequencies. For instance, the wide band gap of GaN enables the material to become intrinsic at a significantly higher temperature. Other desirable characteristics of III nitrides include excellent electron transport properties, high saturated drift velocity [27], strong atomic bonding [21], thermal stability [31, 32], chemical stability [33, 34], high mechanical stability, and high breakdown fields [27], which are required for high-power devices [27]. Gallium nitride's mechanical and electrical properties make it appropriate for use in sensing applications. GaN sensors can operate at higher temperatures due to the high melting point of the material. Additionally, it has a wide, direct band gap. Due to inexpensive materials, the production of GaN resistive sensors is more cost-effective than that of many other types of sensors [35, 36].

2.1 Crystal GaN Can Generally Exist in Two Phases

1) Hexagonal (wurtzite) and
2) Cubic (zinc-blende).
3) Hexagonal Gallium Nitride

The majority of hexagonal GaN is grown on silicon (100), silicon carbide (SiC), or sapphire (0001) substrates. The hexagonal structure predominates under growth conditions characterized by an increase in group V species (e.g., nitrogen) or substrate temperatures exceeding 50 degrees Celsius. In a hexagonal structure, the bonding between the atoms can be seen to form tetrahedrons, with four Ga atoms [37, 38] located at the tetrahedron's extremities and thus at an equal distance to the N atom, which is located at the tetrahedron's center. This form of bonding guarantees that the atoms are tightly packed [39, 40]. Figure (1) below illustrates the atomic structure of hexagonal GaN [41, 42].

2.1.1 Cubic Gallium Nitride

The cubic GaN atomic structure is depicted in Figure. 2 [40]:

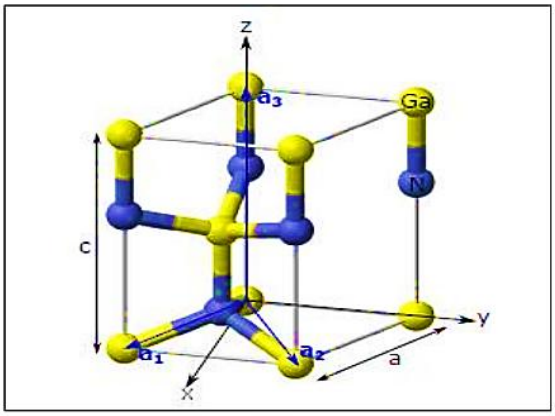

Figure 1. Hexagonal GaN structure [41].

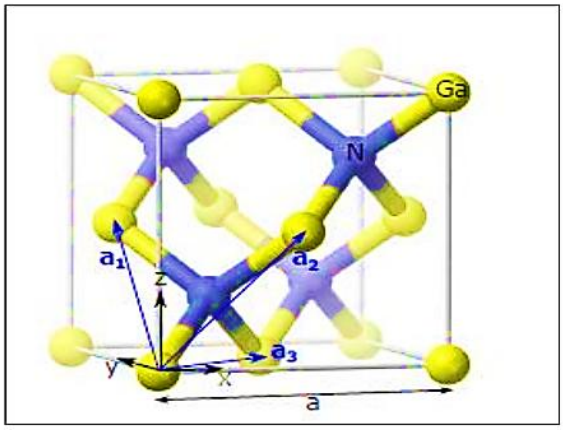

Figure 2. Cubic GaN structure [41].

2.2 Temperature Resistance of Gallium Nitride

To withstand elevated operating temperatures, sensor materials must possess a high melting point. The sensor's materials must be thermally stable in these conditions. The highest melting point corresponds with the highest thermal stability. As shown in Table (1), Gallium Nitride is stable at high temperatures because its melting point is 2700 C^0, which is the temperature at which other semiconductors exist in liquid phase [35].

Table 1 The melting temperatures of a number of semiconductors [35]

Semiconductor materials	Melting point C^0
GaN	2700
Si	937
GaAs	1421

2.3 Electron mobility of Gallium Nitride

Electron mobility (n) is the response of sensors to variations in the conduction of electrons or electron holes in a material. The electron drift velocity (vn) is the average electron velocity caused by the administration of an electric field (E). As demonstrated by flaw Equation [35, 43, and 44], the movement of electrons in electron drift velocity at this field is related to electron mobility

$$\mu n = \frac{vn}{E} \quad (1)$$

For improved conductivity in sensing devices without the risk of a voltage breakdown, electron mobility must be as high as feasible. When a modest change in voltage causes rapid increases in current, breakdown occurs. semiconducting material with a higher n breakdown voltage at lower voltages. As shown in Table (2), GaN has average electron mobility (440 cm2/V s) compared to many other semiconductors. However, the n of GaN is sufficient for sensor function without risk of breakdown at 2.5 V, which is the bias voltage for these investigations [35].

Table 2 Electron mobility of some semiconductors material [35]

Semiconductors material	μ_n (cm^2 /V. s)
GaN	440
Si	1350
SiC	500
GaP	300
ZnS	110

3. GALLIUM NITRATE APPLICATIONS (GAN)

Table 3 below shows that some application of GaN.

Table 3 Applications of GaN

Type of application	Properties
LED	The ratio of Al (AlGaN) or In (InGaN) to GaN affects the color of LEDs and their ability to read Blu-ray discs. Diffusion-assisted carrier injection (DACI) is a method for LEDs based on III-nitride to prevent a drop in efficiency,[45, 46].
Transistors	in the past 12 years, MOSFET and MESFET transistors based on GaN and silicon have been developed. GaN-based power converters have entered the market with lower efficiency and a larger dimension than conventional components. Two-dimensional electron gas (2DEG) has low on-resistance, high current capacities, and high power densities. GaN-based power switching devices include GaN HEMTs, GaN HEMTs in cascade, and lateral GaN MOSFETs in enhancement mode,[47, 48].
Radars	Due to its high voltage, high temperature, and high-frequency characteristics, GaN has been utilized in military electronics and instruments, such as AESA, [49]. In 2018, Lockheed Martin's GaN-funded tactical and operational radars were delivered to Latvia and Romania. Saab has recently tested a novel GaN-based radar on a JAS-39 Gripen fighter. In electronic and optical devices, advanced epitaxial growth techniques such as HEMT, single-electron transistors, laser diodes, and light-emitting diodes require nanometer-scale structures with high precision. HEMT is the semiconductor architecture used to manufacture GaN transistors,[50].
Waveguide	III-Nitride-based WGs fabricated with GaN-AlGaN materials are afflicted with a high density of dislocations and tensile strain, resulting in optical losses,[51, 52].
GaN Photodetector	The GaN photodetector consists of the following photodetector types: • Photoconductive Materials [53] • Schottky barrier photodiodes based on AlGaN [54] • Metal-Semiconductor-Metal (MSM) Photodiodes [53] • Photodiodes p-n, p-i-n, and avalanche [55] • Photographic Transistors [56] • Multiple quantum well (MQW) UV detectors based on nitride [57] • UV photodetectors made from polarization-sensitive GaN [58-60]
Gas Sensor	GaN nanostructures were ideally suited for detecting hydrogen and alcohol, as well as various oxidizing gases. Recently, P-i-n GaN (NRs) Nano rods comprised of InGaN/GaN multi-quantum wells have been recorded for the detection of NO gas [61, 62]. This Nano rod-based species detected NO concentrations as low as 10 ppm at room temperature. Even though the response time was acceptable (180 s), the system recovery process was excessively delayed (400 s) even when exposed to UV light. In addition, owing to the various surface states possessed by InGaN NRs, it exhibited a high degree of selectivity for NO gas over other interfering oxidizing gases, [63, 64].

4. GALLIUM NITRATE GAS SENSOR (GAN)

GaN is a promising material for chemical sensors due to the large band gap and the associated excellent chemical stability and mechanical robustness; these semiconductors can be used in many harsh applications. These include gas sensing operations during the processing of chemical reactors, the detection of fuel leaks in automobiles and aircraft, and onboard fire detectors on aircraft and spacecraft. The ability to integrate a GaN gas sensor with GaN-based solar-blind UV photo detectors or high-power, high-temperature electronic devices on the same chip [65, 66] is a unique advantage of this sensor. Using GaN thin films, various reducing and oxidizing gases can be examined [67, 68]. GaN can operate at temperatures greater than 400 °C and has adequate thermal conductivity in bulk, low-defect wafers, making it a suitable material for gas sensing [69, 70]. Recent reports describe GaN gas sensors with Schottky contacts, in which a catalytic metal such as Pd or Pt facilitates the adsorption of gas atoms on the semiconductor surface to form a polarized layer. This layer alters the electrostatic potential, which modifies the metal work function and, consequently, the effective Schottky barrier height. On the other hand, resistive gas sensors do not rely on the Schottky contacts and specific catalytic metals that are necessary for gas detection. Instead, they take advantage of the variation in near-surface conductivity, which is most likely caused by the adsorption of gas species. Historically, metallic oxide semiconductors such as WO3, SnO2, and ZnO have comprised the majority of resistive gas sensors utilizing a surface conductivity change. In the case of gases containing oxygen, it is believed that the oxygen adsorbs onto the surface of the semiconductor and generates an electron acceptor state within the band gap of p-type semiconductors, while n-type semiconductors generate an electron donor state from reduced gases. Thus, surface adsorption results in a change in the fractional surface coverage of this acceptor/donor state, which can be

detected as a change in conductivity [65, 71]. Table (4) shows Summary of sensing performance of Gallium Nitrate (GaN) based sensors.

Table 4 Summary of sensing performance of Gallium Nitrate (GaN) based sensors

Type of sensor	Type of substrate	Fabrication method	Results
n-ZnO/p-GaN	GaN/sapphire	Atomic layer deposition (ALD)	The researcher examined the properties of n-ZnO/p-GaN heterostructures for possible use in optoelectronic devices. The current voltage characteristics of the heterojunction were favorable, indicating UV detector potential, [72].
Porous GaN	Sapphire	prism coupling	This research demonstrates that nanostructures can provide a positive outlook for III-nitride semiconductors. The refractive index and other optical properties of GaN films can be tailored to create optical devices with precise configurations, [73].
GaN	Sapphire	Pulse laser deposition	The outcome demonstrated that annealing could restore the film's surface. The GaN film becomes extremely flat. Consequently, by modulating the annealing temperature, a highly crystalline, soft, and strain-free GaN film was produced.74]
GaN	Si (111)	Low-cost electrochemical deposition	The GaN on Si (111) substrate was also found to be more sensitive than the GaN on Si (100) substrate. The experimental results suggest that gallium nitride with a gallium oxide face could be used for gas sensing, [75].
GaN (h-GaN)	Si (100) and Si (111)	Pulse laser deposition	The research demonstrated that h-GaN grown on Si (111) has superior crystalline structure and optical properties than that grown on Si (100); the PLD method showed promise for fabricating low-cost GaN-based optoelectronic devices on Si substrates due to the minor mismatch between the Si (111) substrate and h-GaN film orientations, [76].
Gallium nitride (GaN) nanowires	Zinc oxide /silicon substrate (100)	Thermal evaporation	1. SEM images revealed a highly dense GaN NW grown on a high-quality ZnO thin film with flower-shaped nanoparticles. 2. Using X-ray diffraction, GaN and ZnO/Si thin films were shown to have hexagonal wurtzite structures. 3. Photoluminescence (PL) measurements of ZnO/Si revealed a strong peak at 382.84 nm (3.23 eV), whereas GaN/ZnO/Si displayed a strong band edge emission at approximately 338.94 nm (3.0 eV), which is characteristic of GaN NWs. 4. As a result of the quantum confinement of nanocrystal line structure, the energy band gap could expand relative to that of gallium (3.45 eV). [77].
GaN	Si	Thermionic vacuum arc (TVA)	The findings indicated that the TVA method could be used to produce GaN with high-quality films at a reasonable price. Further GaN thin film research utilizing TVA is essential for modernizing and developing next-generation optoelectronic devices and introducing new industrial applications, [78].
GaN-NSs	Si (111)	A PAMBE setup	The research demonstrates that NS with lower stress-strain, no buffer layer, a low aspect ratio, and compatibility with Si-technology can herald a new era of cheaper nanosensors in the future,[79].
Zinc oxide (ZnO)	Si and GaN lattice	Pulse laser deposition	The results also demonstrated that the ZnO buffer layer significantly enhances the crystalline quality of GaN films because ZnO and GaN have strong lattice structures that match comparable lattice parameters ,[80].

GaN	Si (111)	Pulse laser deposition	The analysis revealed that as the number of pulses increases, the formation of structures differs in size and shape. With increasing pulses, the presence of the nitrogen (N) element began to manifest on the surface, indicating the N element. The sensitivity of the GaNSi gas sensor increased in proportion to the NH3 gas concentration. [81].
GaN	Sapphire (Al_2O_3)	Chemical vapor deposition (CVD)	The findings indicate that the investigation confirmed sub-band-gap or defect band emissions; however, the effect of these defect bands on the performance of PEC water splitting has not been studied, and additional research is required. The GaN thin layer on a sapphire substrate is thermally stable and begins to degrade at 950 degrees Celsius. At 0.59 V, the highest photo conversion efficiency and photocurrent density relative to RHE were 0.73 percent and 0.099 mA/cm2, respectively.,[82].
GaN	α–GaOOH precursors	Direct nitridation method	The GaN sensor was 10 times more sensitive to oxygen concentrations of 2.07 wt.% than it was to oxygen concentrations of 2.53 wt.%. It exhibited greater stability and sensitivity than Ga_2O_3 sensor, [83]. .
GaN Nanorods		Simple solvothermal method and a low-temperature nitridation process	The results of material characterization reveal nanorod structures with superior growth orientation. At room temperature, gas sensing tests demonstrate outstanding response, repeatability, and selectivity for n-butanol. Establishing the gas adsorption model and electron depletion layer theory,[84].
GaN nanoparticles		Simple chemical route	The ethanol sensitivity is found to be the highest, with the sensitivity and recovery periods being the shortest. The gas sensor properties of GaN appear to be associated with intrinsic defects that serve as sorption sites for gas molecules, [85].
GaN quantum dots (QDs) film		Metal-organic chemical vapor deposition (MOCVD	With a high electron mobility of 1237.37 $cm^2 V^{-1} s^{-1}$ at room temperature, the GaN QDs film sensor is advantageous for gas sensing. The active sites, carrier mobility, surface energy, chemical activity, granule boundary barrier, and electrical conductivity give the sensor its selectivity, repeatability, stability, and ability to be used more than once,[86].
Gallium nitride (GaN) and indium gallium nitride (InGaN		Solvothermal method	Pure GaN and InGaN show a sensing response of 23.8% and 28.1% for a 200 ppm concentration at 300 K, while nanocomposites of GaN and InGaN show a response of 37.4% and 44.1%. This enhancement in nanocomposites can be attributed to the enhanced conductivity, increased number of gas adsorption sites, and decreased bandgap. These materials have been discovered to be an outstanding option for ammonia gas sensing applications,[87]..
GaN nanorods	n-Si(111)	Plasma-assisted molecular beam epitaxy (PA-MBE)	NO gas sensing measurements showed H_2O_2-treated GaN NRs had a four-fold higher response to 100 ppm of NO gas concentration at 50°C. They also responded more strongly to UV illumination, generating electron-hole pairs and causing an elevated NO gas response,[88]..
ZnO	GaN	Electrodeposition	FZnO/GaN nanosheets on GaN form a 55 nm-thick ZnO nanosheet, providing exceptional sensitivity for ethanol detection. This material has faster response times, superior selectivity, and stability, with a detection limit of 100 ppb. The enhancement is mainly due to FZnO and GaN conductivity,[89].
GaN	Si (111)	Chemical vapor deposition (CVD)	The GaN/Si-NPA gas sensor demonstrated effective sensing responses of 1.22 and 1.92–5 ppm at 350°C, with recovery rates of eight and seven seconds for 500

			ppm methanol. The sensor's high specific surface area and active sites make it a promising sensing candidate for methanol detection,[90].

5. TYPES OF GALLIUM NITRATE GAS SENSOR

A wide band gap with low activation energy is the main design parameter for semiconductor gas sensors because it eliminates the influence of ambient temperature on device degradation. Due to their high chemical stability and high melting points, both SiC and GaN serve as materials for the design of sensors for severe environments. Furthermore, GaN possesses high mobility, a high breakdown field, and a high switching speed. [91-93].

5.1 GaN-resistor Sensors

Hydrogen peroxide (H2O2) treatment of GaN can improve sensing performance. Heterostructures, doping, and noble metals increase gas adsorption sites. H2O2 treatment enhanced pure GaN Nano rod sensor responsiveness to 19.4% for 100 ppm NO from 5.35%. UV irradiation caused GaN surface flaws with more electron hole pairs, increasing the response by 29%. The treatment temperature restricts the GaN surface's OH concentration, which affects sensor performance. The device responded 24.24% at 40 °C and 12.52% at 60 °C for 100 ppm NO. 125 Fig. 20 shows a flower-like ZnO ethanol gas sensor with a response or recovery time of 12 s or 9 s. The sensor responded 26.9 to ethanol but less than 4 to other gases. The sensor responded less as the relative humidity increased. Figures 3a–3f exhibited sensor responsiveness, response/recovery time, stability, selectivity, and humidity response at various concentrations. The morphology and heterojunction of flower-ZnO and GaN improved sensor performance since the bare flower-ZnO produced a sensor response of 16.8 while the heterojunction response was 26.9 for 50 ppm at ambient temperature [94, 95]. A layer transfer-based n-MoS2/p-GaN NOx gas sensor was designed and analyzed. At 27 °C and 50 ppm NO concentration, heterojunction responses were 28.7%, 50%, and 98.42%, respectively. At ambient temperature, n-MoS2/p-GaN responded 9.6 times and 3.2 times higher than bare p-GaN and n-MoS2, respectively. UV illumination increased sensor responsiveness (64.67% for NO at 50 ppm) by 2.32 times. UV illumination reduced response and recovery time from 290 s (1310 s) to 235 s (800 s) [96, 97]. Due to its increased active sites, graphene with oxygen functional groups improves sensor gadget performance. With Au nanoparticles, a CO gas sensor with rGO on GaN responded 35% (20 ppm) at 50 ppm. Increased active sites in the Au@rGO/GaN hybrid structure boost CO and oxygen ion interactions, improving sensor performance [98, 99]. High-temperature GaN-based hydrogen sensors were made by direct nitridation. They found that GaN sensor sensitivity increased by 10 times with 2.07 wt% oxygen content compared to 1.9 wt% and decreased beyond 2.53 wt%. Oxygen lowered GaN mobility and conductivity, affecting sensitivity [100, 101]. The ZnO NRs/GaN heterojunction H2S gas sensor responded at 51.3 ppm for 50 ppm at 240 °C, 2.83 times greater than bare ZnO. Heterojunctions with more oxygen vacancy sites and GaN-enhanced electron transport improve sensor performance [102, 103]. Pt and Pd-adorned GaN nanowires for hydrogen sensing by chemical vapor deposition were compared. Pt-GaN responded 1.44% at 150 °C and 8.96% at 200 °C to 400 ppm H2. Pd ornamentation had the highest reaction because it had less quenching and more charge carriers [104, 105]. Temperature and gas concentration improved the InGaN/GaN MQW NO gas sensor response. Due to device surface reactivity, the 100 ppm NO gas response was 10.14% at 35 °C and 222.14% at 200 °C. Since desorption exceeded adsorption at high temperatures, response and recovery times decreased. From 10.14% (no light) to 120% with 20 mW cm2 UV intensity [106, 107]. At 10 ppm NO2, the Ga2O3-core/ZnO-shell nanorod heterojunction response was 181 times greater than the bare structure, with values of 7,246.66% (Ga2O3-ZnO), 40.31% (Bare-Ga2O3), and 10.52% (Bare-ZnO) [108, 109]. The hybrid NO2 sensor based on TiO2 and GaN showed that the sensor response and sensitivity depended on TiO2 thickness and doping concentration [110, 111].

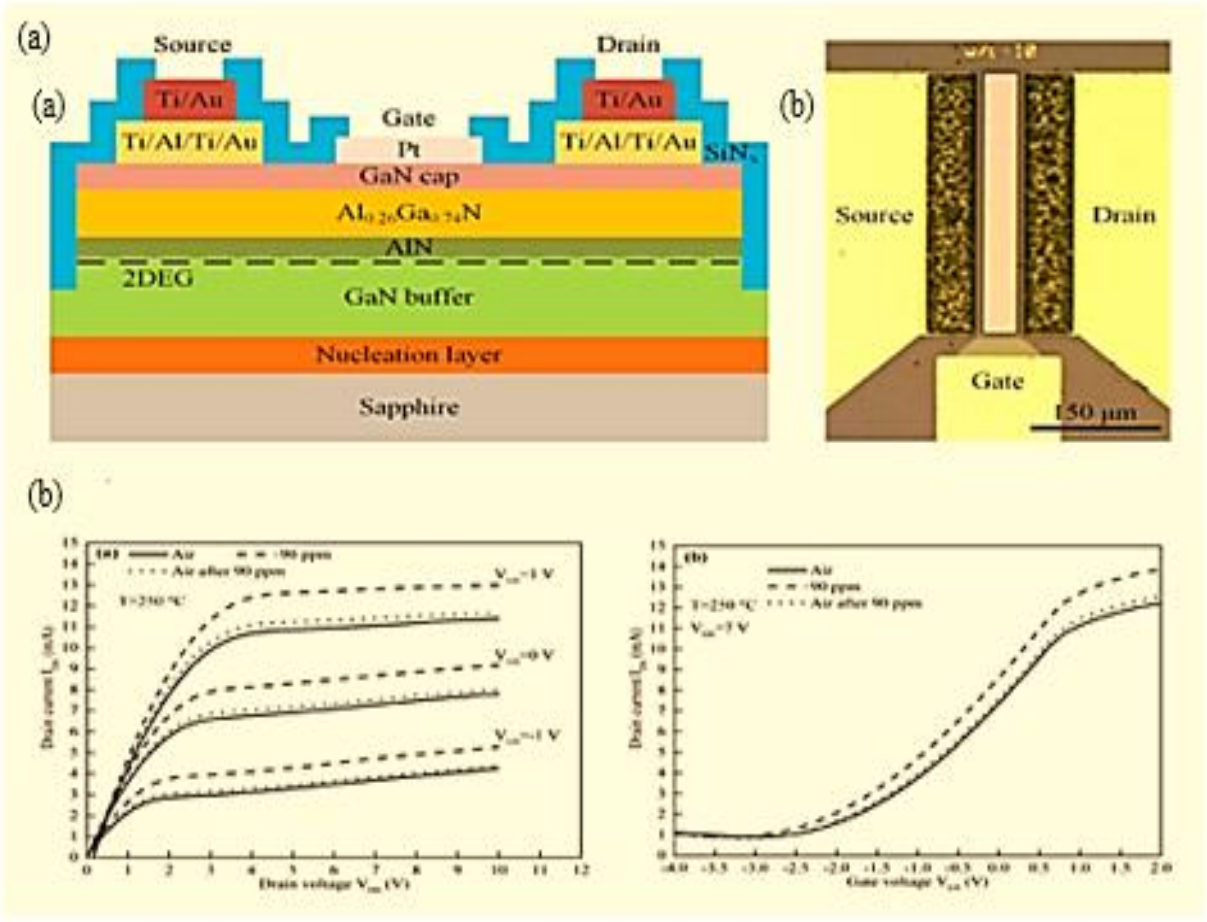

Figure 3. (a) RT resistance curves for C2H5OH concentrations. (b) 50 ppm C2H5OH response and recovery time at RT (c) Sensor behavior when C2H5OH concentration is rapidly varied between 50 ppm and the ambient environment at RT. (d) FZnO/GaN sensor gas responses (e) 30-day sensor cycling stability (f) Response to C2H5OH at 0, 33, 57, and 76% RH. Ref. [94]. allowed the reproduction of this figure.

5.2GaN-schottky Diode Sensors

Pt-decorated GaN Schottky diode hydrogen sensors performed better than Pd ones. Figure (4) shows that the device's sensing capability decreases with greater temperature and positive bias voltage. The Pt-GaN Schottky diode responded 1.03 × 105 with 15 s/19 s at 300 k with 1 ppm concentration [110]. A hydrogen Schottky diode sensor containing GaN, a nickel oxide (NiO) layer, and palladium has a response of 8.1 × 103 at 0.25 V and 1.8 × 104 at 2 V [112, 113]. GaOx or AlGaOx oxide layers enhanced sensors in numerous studies. Another hydrogen GaN Schottky diode sensor created by hydrogen peroxide (H2O2) treatment and electroless plating (EP) has a 5.5 × 106 response and a 22 s/21 s response/recovery time at 300 K [114, 115]. Hafnium oxide (HfO2) hydrogen sensors responded 4.9 × 105 with a response/recovery time of 39 s/42 s at 300 K. HfO2 reduced leakage current from 1.81 × 10 8 A to 4.55 × 10 10 A, improving responsiveness [116, 117]. An ammonia (NH3) sensor based on a GaN Schottky device with Pt and GaOx dielectric reduced leakage current from 1.5 × 108 A to 2.1 × 1011 A, improving sensor performance. 1000 ppm response was 252, with a response/recovery time of 288 s/120 s at 473 K [118, 119]. A Schottky diode ammonia sensor using AlGaN/GaN heterostructures with ZnO nanorod functionalization identified a lower limit of 0.1–2 ppm between 25 °C and 300 °C. For 2 ppm ammonia at 25–300 °C, the device's sensitivity increased from 3.36% to 12.59%. Recovery time reduced from 60 s to 25 s as the temperature increased from 25 °C to 300 °C, whereas response time was around 10 s over the whole temperature range [120, 21] Chemical vapor deposition produced another Schottky diode gas sensor for H2S detection based on Pt/GaN. The sensor responded with 14.62 A ppm at 0.1–1 ppm and 5.844 at 1–10 ppm. Since higher gas concentrations reduced the Pt/GaN binding site, sensor performance degraded [122, 123]. An AlGaN/GaN Schottky diode-based ethanol gas sensor with silver deposition had a 45.4% current change at 0.9 V forward bias. [124, 125] The Pd/ZnO/GaN heterojunction Schottky diode NOx sensor also showed a larger current change for low gas concentrations. Schottky contact and heterojunction morphology lowered the detection limit to 1 mA for < 10 ppm NO2[126, 127]

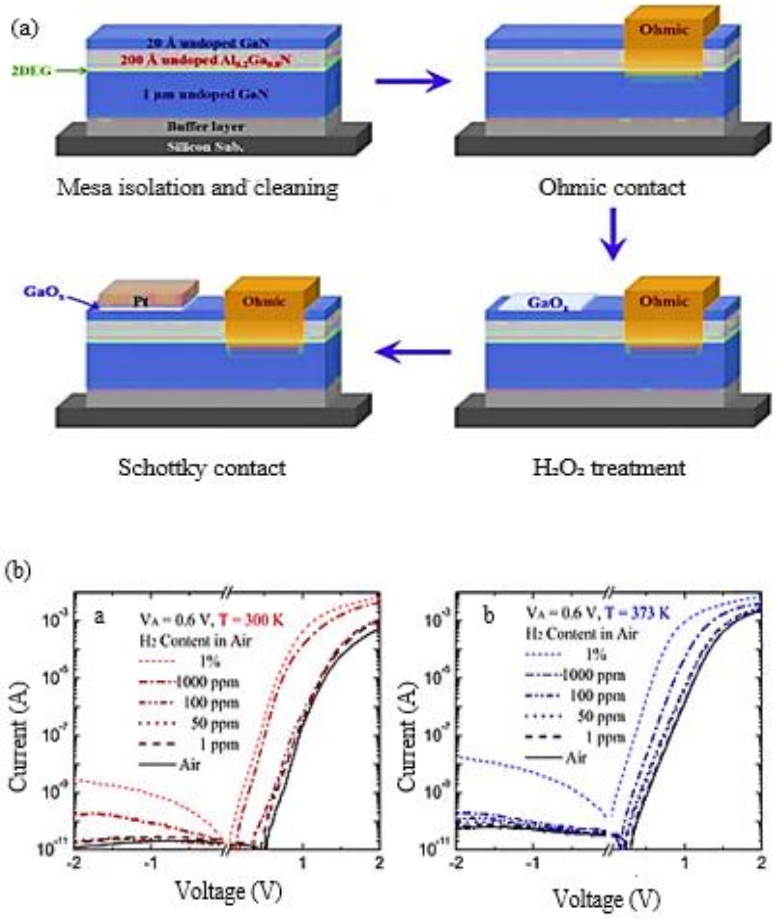

Figure 4. (a) Pt/GaOx/GaN Schottky diode fabrication flowchart (b) Current-voltage (I-V) characteristics of the device at 300 and 373 hydrogen gas concentrations Ref. [120]. gave permission to reproduce this figure.

5.3 GaN-fet Sensors

In 1975, the first FET-based H2 sensor was discovered. Transducer improvements improved sensor performance. Few are suspended gate FETs with and without hybrid materials, capacitive controlled FETs, floating gate FETs, and dual gate FETs. GaN superseded Silicon for high-temperature applications due to its wider band gap and greater thermal and electrical resistance. High-temperature H2S sensors use AlGaN or GaN HEMTs with Pt gates. In Figure (5), the test gas affected the drain current and threshold voltage. At 200 °C, 90 ppm H2S, 1 V gate voltage, and 2.17 mA drain current change, the response/recovery time was 476 s/1316 s. Response and recovery fell to 219 s/507 s at 250 °C. H2S sensing was 22% higher than H2's 4.88%. H2 pre-treatment enabled [128, 129]. AlGaN/GaN HEMT sensors with Pt gates to detect 30–90 ppm at 250 °C. [130, 131]. AlGaN/GaN HEMT hydrogen sensors with functionalized Pt gates were tested for high temperature and radiation susceptibility. At 200–350 °C, the sensor sensitivity increased from 16–33%, resulting in better performance. The sensor also withstood high radiation after 1015/cm2 at 5 MeV proton-irradiation [132, 133]. AlGaN/GaN HEMT sensors with SnO2 gates detected 1% oxygen and nitrogen at 100 °C [134]. The integrated IZO-gated AlGaN/GaN HEMT O_2 sensor recognized oxygen at low temperatures, unlike oxide-based oxygen sensors.

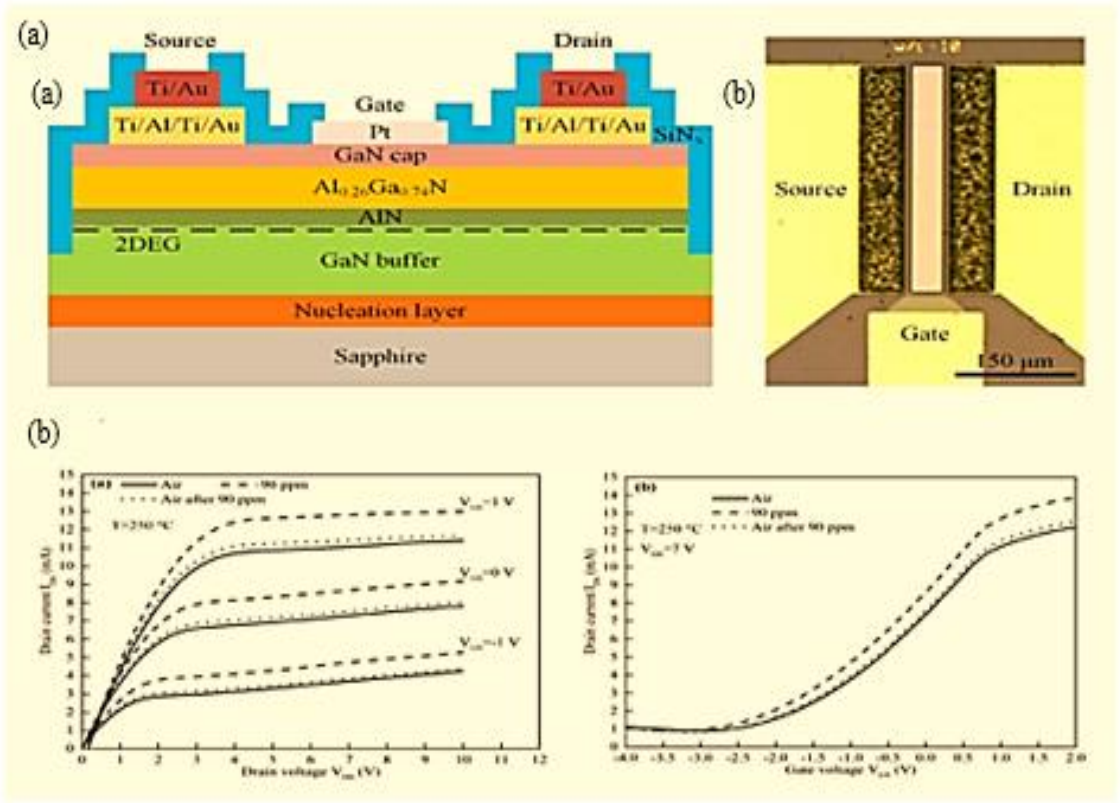

Figure 5. (a) Pt-AlGaN/GaN HEMT H2S sensor cross-section (b) Top-view optical micrograph of sensor fabrication (b) (a) Output (IDS-VDS) and transfer (IDS-VGS) characteristics of the Pt-HEMT sensor before and after exposure to 90 ppm H_2S at 250 °C Ref. [131]. allows reproduction of this figure.

6. CONCLUSION

This paper provided an overview of the majority of studies that employed gallium nitride-based gas sensors with varying layer thicknesses and substrate materials for a variety of applications. It was observed that the gas sensor based on gallium nitride material provided a technical advancement and covered a wide range of sensing application fields, as well as having the potential to improve optoelectronic device parameters such as high performance, high speed, low cost, high detecting sensitivity, and compact size, thereby enhancing quality, reliability, and economic efficiency.

REFERENCES

[1] L. Novotny and B. Hecht, Cambridge University Press,(2006).

[2] Tamara E Abdulrahman, Evan T Salim, Rana O Mahdi and MHA Wahid, Nb2O5 nano and microspheres fabricated by laser ablation, Advances in Natural Sciences: Nanoscience and Nanotechnology, Volume 13, Number4, 045006 (2022), DOI 10.1088/2043-6262/ac99cf.

[3] C. P. Poole, Jr. and F. J. Owens, John Wiley & Sons, Inc., Hoboken, New Jersey, (2003).

[4] Fatema H. Rajab, Rana M. Taha, Aseel A. Hadi, Khawla S. Khashan & Rana O. Mahdi , Laser induced hydrothermal growth of ZnO rods for UV detector application, Opt Quant Electron 55, 208 (2023). https://doi.org/10.1007/s11082-022-04473-2.

[5] Y. GogotsiCRC Press Taylor & Francis Group, (2006).

[6] Evan T. Salim, Rana O. Mahdi, Doaa Mahmoud, Subash C. B. Gopinath & Motahher A. Qaeed, Effect of Laser Wavelength on the Structural, Morphological, and Optical Plasmonic Properties of Au@WO3 Core–Shell NPs, Plasmonics (2025). https://doi.org/10.1007/s11468-025-02929-1.

[7] P. M. Aneesh, Ph.D. Thesis, Cochin University of Science and Technology, (2010).

[8] Jurn Y. N.; Malek F.; Mahmood S. A.; Liu W.-W.; Fakhri M. A.; Salih M. H., Modelling and simulation of rectangular bundle of single-walled carbon nanotubes for antenna applications Key Engineering Materials, 701, 57-66 (2016) 10.4028/www.scientific.net/KEM.701.57.

[9] G. Sankar, A. Claude, S. Sathya and A. Poiyamozhi, Advances in Applied Science Research, 4(6), pp. 13-20, (2013).

[10] Azzam Y. Kudhur, Evan T. Salim, Ilker Kara, Makram A. Fakhri & Rana O. Mahdi, Structural optical and morphological properties of copper oxide nanoparticles ablated using pulsed laser ablation in liquid, J Opt 53, 1936–1945 (2024). https://doi.org/10.1007/s12596-023-01331-6.

[11] K. Buchholt, Ph.D. Thesis, Linköping University, Sweden, (2011).

[12] Salim Z. T.; Hashim U.; Arshad M. K. M.; Fakhri M. A., Simulation, fabrication and validation of surface acoustic wave layered sensor based on ZnO/IDT/128° YX LiNBO3, International Journal of Applied Engineering Research, 11(15), 8785-8790 (2016).

[13] H. S. Hassan, A. B. Kashyout, I. Morsi, A. A. A. Nasser, and A. Raafat, American Institute of Physics, 978-0-7354-1295-8, 020042, pp. 1-9, (2015).

[14] Ismail R. A.; Salim E. T.; Hamoudi W. K., Characterization of nanostructured hydroxyapatite prepared by Nd:YAG laser deposition, Materials Science and Engineering C, 33(1), 47-52 (2013) 10.1016/j.msec.2012.08.002.

[15] H. W. Kim and N. H. Kim, Applied Surface Science, 236, pp.192–197,(2004).

[16] Jurn Y. N.; Malek F.; Mahmood S. A.; Liu W.-W.; Gbashi E. K.; Fakhri M. A., Important parameters analysis of the single-walled carbon nanotubes composite materials, ARPN Journal of Engineering and Applied Sciences, 11(8), 5108-5113 (2016).

[17] T. D Moustakas and R. Paiella, Rep. Prog. Phys. 80 106501, pp.1-41, (2017).

[18] Khawla S. Khashan, Aseel A. Hadi, Rana O. Mahdi & Doaa S. Jubair, Aluminum-doped zinc oxide nanoparticles prepared via nanosecond Nd: YAG laser ablation in water: optoelectronic properties, Opt Quant Electron 56, 125 (2024). https://doi.org/10.1007/s11082-023-05630-x.

[19] M. Yang, H. S. Ahn, J. H. Chang, S. N. Yi, K. H. Kim and H. Kim, Journal of the Korean Physical Society, Vol. 43, No. 6, pp. 1087_1090,(2003).

[20] Evan T. Salim, Rana O. Mahdi, Doaa Mahmoud, Subash C. B. Gopinath & Forat H. Alsultany, An Analysis Study Employing Laser Ablation in Gold Colloidal at Different Numbers of Laser Pulses, Plasmonics (2025). https://doi.org/10.1007/s11468-025-02998-2.

[21] F. C. Yong, Ph.D. Thesis, Universiti Sains Malaysia, (2016).

[22] Hattab F.; Fakhry M., Optical and structure properties for nano titanium oxide thin film prepared by PLD, 2012 1st National Conference for Engineering Sciences, FNCES 2012, 6740474 (2012) 10.1109/NCES.2012.6740474.

[23] L. He, Ph.D. Thesis, Virginia Commonwealth University, (2004).

[24] Azzam Y. kudhur, Evan T. Salim, Ilker Kara, Rana O. Mahdi & Raed K. Ibrahim, The effect of laser energy on Cu2O nanoparticles formation by liquid-phase pulsed laser ablation, J Opt 53, 1309–1321 (2024). https://doi.org/10.1007/s12596-023-01319-2.

[25] T. Zhang, T. Sugiura, W. Lu, F.Wu, J. Mao, P. Qiu and Hugejile, Journal of The Ceramic Society of Japan, 125[4], pp. 371- 374, (2017).

[26] Fakhri M. A.; Al-Douri Y.; Hashim U., Fabricated Optical Strip Waveguide of Nanophotonics lthium Niobate, IEEE Photonics Journal, 8(2), 7409919 (2016) 10.1109/JPHOT.2016.2531583.

[27] R. B. Radzali, Ph.D. Thesis, Institute of Nano Optoelectronics Research and Technology (INOR) USM, (2017).

[28] Abdul Muhsien M.; Salem E.T.; Agool I.R., Preparation and characterization of (Au/n-Sn O2 /Si O2 /Si/Al) MIS device for optoelectronic application, International Journal of Optics, 2013, 756402 (2013) 10.1155/2013/756402.

[29] G N. Chaudhari, V. R. Chinchamalatpure and S. A. Ghosh, , American Journal of Analytical Chemistry, 2, pp. 984-988, (2011).

[30] Rana O. Mahdi, Aseel A. Hadi, Juhaina M. Taha, Khawla S. Khashan, Preparation of nickel oxide nanoparticles prepared by laser ablation in water, AIP Conf. Proc. 2213, 020309 (2020) https://doi.org/10.1063/5.0000116.

[31] C. C. Woei Ph.D. Thesis, Universiti Sains Malaysia, (2017).

[32] Hassan M. A. M.; Al-Kadhemy M. F. H.; Salem E. T., Effect irradiation time of Gamma ray on MSISM (Au/SnO2/SiO2/Si/Al) devices using theoretical modeling, International Journal of Nanoelectronics and Materials, 8(2), 69-82 (2015).

[33] A. R. Isroi, Conference Paper, 10.13140/RG.2.1.2837.9602, (2015).

[34] Fakhri M. A.; Salim E. T.; Wahid M. H. A.; Hashim U.; Salim Z. T.; Ismail R. A., Synthesis and characterization of nanostructured LiNbO3 films with variation of stirring duration, Journal of Materials Science: Materials in Electronics, 28(16), 11813-11822 (2017) 10.1007/s10854-017-6989-0.

[35] C. N. Monteparo, MSc thesis, University of South Florida, (2009).

[36] Roaa A. Abbas, Evan T. Salim & Rana O. Mahdi, Deposition time effect on copper oxide nano structures, an analysis study using chemical method, J Mater Sci: Mater Electron 35, 427 (2024). https://doi.org/10.1007/s10854-024-12143-0.

[37] M. E. A. B. Samsudin, MSc thesis, Universiti Sains Malaysia, (2016).

[38] Fakhri M. A.; Wahid M. H. A.; Badr B. A.; Kadhim S. M.; Salim E. T.; Hashim U.; Salim Z. T., Enhancement of Lithium Niobate nanophotonic structures via spin-coating technique for optical waveguides application, EPJ Web of Conferences, 162, 1004 (2017) 10.1051/epjconf/201716201004.

[39] K. W. Mah, Ph.D. Thesis, School of Physical Sciences Dublin City University, (2002).117.

[40] Fakhri M. A.; Numan N. H.; Mohammed Q. Q.; Abdulla M. S.; Hassan O. S.; Abduljabar S. A.; Ahmed A. A., Responsivity and response time of nano silver oxide on silicon heterojunction detector, International Journal of Nanoelectronics and Materials, 11(Special Issue BOND21), 109-114 (2018).

[41] T. Aunsborg and R. Hjelmgart MSc thesis, Aalborg University, (2016).

[42] Evan T. Salim, Ahmed T. Hassan, Rana O Mahdi, Forat H. Alsultany, Physical Properties of HfO2 Nano Structures Deposited using PLD, IJNeaM, vol. 16, no. 3, pp. 495–510, Oct. 2023.

[43] Salim E. T.; Saimon J. A.; Abood M. K.; Fakhri M. A., Some physical properties of Nb2O5 thin films prepared using nobic acid based colloidal suspension at room temperature, Materials Research Express, 4(10), 106407 (2017) 10.1088/2053-1591/aa90a6.

[44] Roaa A. Abbas, Evan T. Salim, and Rana O. Mahdi, Study based on micro-and nanosized raw materials using the hydrothermal method, International Journal of Nanoelectronics and Materials (IJNeaM)Volume 18, No. 1, January 2025 [141-149]. https://doi.org/10.58915/ijneam.v18i1.1751.

[45] H. Morkoc, S. Strite, G. B. Gao, M. E. Lin, B. Sverdlov, and M. Burns, J. Appl. Phys., vol. 76, no. 3, pp. 1363–1398, 1994.

[46] O. A. Abdulrazaq and E. T. Saleem, Turkish J. Phys., vol. 30, no. 1, pp. 35–40, 2006.

[47] Zainab T. Hussain, Khawla S. Khashan, Rana O. Mahdi, Characterization of cadmium oxide nanoparticles prepared through Nd:YAG laser ablation process, Materials Today: ProceedingsVolume 42, Pages 2645 – 26482021. https://doi.org/10.1016/j.matpr.2020.12.594.

[48] S. Davis, Power Electron. Technol., vol. 35, no. 11, pp. 39–40, 2009.

[49] E. T. Salim, A. I. Hassan, and S. A. Naaes, Mater. Res. Express, vol. 6, no. 8, p. 86416, 2019.

[50] N. Iizuka, K. Kaneko, and N. Suzuki, J. Appl. Phys., vol. 99, no. 9, p. 93107, 2006.

[51] R. Hui, Y. Wan, J. Li, S. Jin, J. Lin, and H. Jiang, IEEE J. Quantum Electron., vol. 41, no. 1, pp. 100–110, 2005.

[52] E. Monroy, F. Calle, E. Munoz, F. Omnès, B. Beaumont, and P. Gibart, J. Electron. Mater., vol. 28, no. 3, pp. 240–245, 1999.

[53] E. Monroy, F. Calle, E. Munoz, F. Omnes, P. Gibart, and J. A. Munoz, Appl. Phys. Lett., vol. 73, no. 15, pp. 2146–2148, 1998.

[54] J. C. Carrano et al., Electron. Lett., vol. 34, no. 7, pp. 692–694, 1998.

[55] W. Yang, T. Nohava, S. Krishnankutty, R. Torreano, S. McPherson, and H. Marsh, Appl. Phys. Lett., vol. 73, no. 7, pp. 978–980, 1998.

[56] F. Omnès, E. Monroy, E. Muñoz, and J.-L. Reverchon, in Gallium Nitride Materials and Devices II, 2007, vol. 6473, p. 64730E.

[57] Evan T. Salim, Rana O. Mahdi, Tamara E. Abdulrahman, Makram A. Fakhri, Jehan A. Siamon, Ahmad S. Azzahrani & Subash C.B. Gopinath, RE-crystallization of Nb2O5 nanocrystals: a study employing different laser wavelength, J Opt (2024). https://doi.org/10.1007/s12596-024-01942-7.

[58] Fakhri M. A.; Salim E. T.; Wahid M. H. A.; Hashim U.; Salim Z. T., Optical investigations and optical constant of nano lithium niobate deposited by spray pyrolysis technique with injection of Li2CO3 and Nb2O5 as raw materials, Journal of Materials Science: Materials in Electronics, 29(11), 9200-9208 (2018) 10.1007/s10854-018-8948-9.

[59] M. Reddeppa et al., Dalt. Trans., vol. 48, no. 4, pp. 1367–1375, 2019.

[60] Aseel A. Hadi, Juhaina M. Taha, Rana O. Mahdi, Khawla S. Khashan, Influence of laser pulse on properties of NiO NPs prepared by laser ablation in liquid, AIP Conf. Proc. 2213, 020308 (2020) https://doi.org/10.1063/5.0000115.

[61] V. Popa, I. M. Tiginyanu, V. V Ursaki, O. Volcius, and H. Morkoç, Semicond. Sci. Technol., vol. 21, no. 12, p. 1518, 2006.

[62] Fakhri M. A.; Al-Douri Y.; Bouhemadou A.; Ameri M., Structural and Optical Properties of Nanophotonic LiNbO3 under Stirrer Time Effect, Journal of Optical Communications, 39(3), 297-306 (2018) 10.1515/joc-2016-0159.

[63] F. Yun, S. Chevtchenko, Y. Moon, and H. Morkoç, Appl. Phys. Lett. 87, 073507,pp. 1-3 (2005).

[64] Evan T. Salim, Roaa A. Abbas, Raed K. Ibrahim, Rana O. Mahdi, Makram A. Fakhri, Ahmad S. Azzahrani, Forat H. Alsultany, Subash C. B. Gopinath & Zaid T. Salim, Impact of Decoration Method on Some Physical Properties of Ag@Cu2O Nanostructure, Plasmonics (2024). https://doi.org/10.1007/s11468-024-02569-x.

[65] X. Luoa, X. Zhenga, D. Wang, Y. Zhang, H. Cheng, X. Wang, H. Zhuang and Y. Lou, Sensors and Actuators, B 202, pp. 1010–1018, (2014).

[66] Khawla S khashan, Rana O Mahdi, Ban A. Badr, Farah Mahdi, Preparation and characterization of ZnMgO nanostructured materials as a photodetector, Journal of Physics: Conference Series 1795 (2021) 012008. doi:10.1088/1742-6596/1795/1/012008.

[67] J. S. Wright, Wantae Lim, D P Norton, S J Pearton1, F Ren, Jason L Johnson and Ant Ural, "Nitride and oxide semiconductor nanostructured hydrogen gas sensors", Semicond. Sci. Technol. 25 024002 (8pp), pp.1-8, (2010).

[68] Roaa A. Abbas, Evan T. Salim & Rana O. Mahdi, Morphology transformation of Cu2O thin film: different environmental temperatures employing chemical method, J Mater Sci: Mater Electron 35, 1057 (2024). https://doi.org/10.1007/s10854-024-12823-x

[69] Fakhri M. A.; Wahid M. H. A.; Kadhim S. M.; Badr B. A.; Salim E. T.; Hashim U.; Salim Z. T., The structure and optical properties of Lithium Niobate grown on quartz for photonics application, EPJ Web of Conferences, 162, 1005 (2017) 10.1051/epjconf/201716201005.

[70] L. Wachnicki, S. Gieraltowska, B. S. Witkowski, S. Figge, D. Hommel, E. Guziewicz and M. Godlewski, , Acta Physica Polonica A, Vol. 124, pp 869- 872, (2013).

[71] B. Alshehri et al., Appl. Phys. Lett., vol. 105, no. 5, p. 51906, 2014.

[72] Y.-W. Cheng, H.-Y. Wu, Y.-Z. Lin, C.-C. Lee, and C.-F. Lin, Thin Solid Films, vol. 577, pp. 17–25, 2015.

[73] K. Al-Heuseen, International Journal of Thin Films Science and Technology, 5, No. 2, pp. 113-119, (2016)

[74] W.-K. Wang and M.-C. Jiang, Jpn. J. Appl. Phys., vol. 55, no. 9, p. 95503, 2016.

[75] A. Ramizy, Journal of kufa -physics, Vol.9, No.1 pp. 97-104, (2017).
[76] M. Kundakçı, A. Mantarcı, and E. Erdoğan, Mater. Res. Express, vol. 4, no. 1, p. 16410, 2017.
[77] L. Goswami, R. Pandey, and G. Gupta, Appl. Surf. Sci., vol. 449, pp. 186–192, 2018.
[78] J. He, S. Yang, and Q. Wei, J. Photonic Mater. Technol., vol. 5, no. 1, pp. 1–4, 2019.
[79] Z. E. Slaiby and A. Ramizy, J. Optoelectron. Biomed. Mater. Vol, vol. 12, no. 1, pp. 17–23, 2020.
[80] Y. Pal, M. A. Raja, M. Madhumitha, A. Nikita, and A. Neethu, Optik (Stuttg)., vol. 226, p. 165410, 2021.
[81] A. Hermawan, Y. Asakura, M. Kobayashi, M. Kakihana, and S. Yin, "High temperature hydrogen gas sensing property of GaN prepared from A-GaOOH," Sensors Actuators, B Chem., vol. 276, no. August, pp. 388–396, 2018.
[82] S. Han, Y. Fu, D. Li, D. Han, and Q. Sun, "GaN Nanorods Gas Sensor for Highly Sensitive n-butanol Detection at room Temperature," Electron. Mater. Lett., vol. 19, no. 3, pp. 309–315, 2023.
[83] B. Chitara, D. J. Late, S. B. Krupanidhi, and C. N. R. Rao, "Room-temperature gas sensors based on gallium nitride nanoparticles," Solid State Commun., vol. 150, no. 41–42, pp. 2053–2056, 2010.
[84] D. Han et al., "Conductometric nitrogen dioxide gas sensor based on gallium nitride quantum dots film," Sensors Actuators B Chem., vol. 379, no. December 2022, p. 133197, 2023.
[85] B. Manavaimaran and S. B. Ravichandran, "GaN and InGaN Based Nanocomposites for Ammonia Gas Sensing Applications," Phys. Status Solidi Basic Res., vol. 259, no. 2, pp. 1–10, 2022.
[86] M. Reddeppa, T. K. Phung Nguyen, B. G. Park, S. G. Kim, and M. D. Kim, "Low operating temperature NO gas sensors based hydrogen peroxide treated GaN nanorods," Phys. E Low-Dimensional Syst. Nanostructures, vol. 116, p. 113725, 2020.
[87] C. Wang et al., "In situ synthesis of flower-like ZnO on GaN using electrodeposition and its application as ethanol gas sensor at room temperature," Sensors Actuators, B Chem., vol. 292, no. March, pp. 270–276, 2019.
[88] H. F. Ji et al., "High-performance methanol sensor based on GaN nanostructures grown on silicon nanoporous pillar array," Sensors Actuators, B Chem., vol. 250, pp. 518–524, 2017.
[89] S. J. Pearton et al., J. Appl. Phys., 93, 1 (2003).
[90] G. Korotcenkov, Materials Science and Engineering: B, 139, 1 (2007).
[91] J. Schalwig, G. Müller, M. Eickhoff, O. Ambacher, and M. Stutzmann, Materials Science and Engineering: B, 93, 207 (2002).
[92] C. Wang, Z.-G. Wang, R. Xi, L. Zhang, and G.-B. Pan, Sensors Actuators B, 292,270 (2019).
[93] Jabbar H. D.; Fakhri M. A.; Jalal Abdulrazzaq M., Gallium Nitride -Based Photodiode: A review, Materials Today: Proceedings, 42, 2829-2834 (2021) 10.1016/j.matpr.2020.12.729.
[94] M. Reddeppa, B.-G. Park, G. Murali, S. H. Choi, and M.-D. Kim, Sensors Actuators B, 308, 127700 (2020).
[95] Abdul Amir H. A. A.; Fakhri M. A.; Abdulkhaleq Alwahib A., Review of GaN optical device characteristics, applications, and optical analysis technology, Materials Today: Proceedings, 42, 2815-2821 (2021) 10.1016/j.matpr.2020.12.727.
[96] M. Reddeppa, S. Babu Mitta, T. Chandrakalavathi, B.-G. Park, and M.-D. Kim, Curr. Appl Phys., 19, 938 (2019).
[97] Abdul Amir H. A. A.; Fakhri M. A.; Alwahib A. A.; Salim E. T., Optical Investigations of GaN Deposited Nano Films Using Pulsed Laser Ablation in Ethanol, International Journal of Nanoelectronics and Materials, 15(2), 129-138 (2022).
[98] A. Hermawan, Y. Asakura, M. Kobayashi, M. Kakihana, and S. Yin, Sensors Actuators B, 276, 388 (2018).
[99] Abdul Amir H. A. A.; Fakhri M. A.; Alwahib A. A.; Salim E. T.; Alsultany F. H.; Hashim U., Synthesis of gallium nitride nanostructure using pulsed laser ablation in liquid for photoelectric detector, Materials Science in Semiconductor Processing, 150, 106911 (2022) 10.1016/j.mssp.2022.106911.
[100] C. Wang, L.-J. Wang, L. Zhang, R. Xi, and G.-B. Pan, J. Alloys Compd., 790, 363(2019).
[101] Jabbar H. D.; Fakhri M. A.; AbdulRazzaq M. J., Synthesis Gallium Nitride on Porous Silicon Nano-Structure for Optoelectronics Devices, Silicon, 14(18) 12837-12853 (2022) 10.1007/s12633-022-01999-8.
[102] A. K. Prasad, P. K. Sahoo, S. Dhara, S. Dash, and A. K. Tyagi, Mater. Chem. Phys., 211, 355 (2018).
[103] Fakhri M. A.; AbdulRazzaq M. J.; Jabbar H. D.; Salim E. T.; Alsultany F. H.; Hashim U., Fabrication of UV photodetector based on GaN/ Psi heterojunction using pulse laser deposition method: Effect of different laser wavelengths, Optical Materials, 137, 113593 (2023) 10.1016/j.optmat.2023.113593.
[104] M. Reddeppa, B.-G. Park, N. D. Chinh, D. Kim, J.-E. Oh, T. G. Kim, and M.- D. Kim, Dalton Trans., 48, 1367 (2019).
[105] Fakhri M. A.; Jabbar H. D.; AbdulRazzaq M. J.; Salim E. T.; Azzahrani A. S.; Ibrahim R. K.; Ismail R. A., Effect of laser fluence on the optoelectronic properties of nanostructured GaN/porous silicon prepared by pulsed laser deposition, Scientific Reports, 13(1), 21007 (2023) 10.1038/s41598-023-47955-3.
[106] C. Jin, S. Park, H. Kim, and C. Lee, Sensors Actuators B, 161, 223 (2012).
[107] Fakhri M. A.; Jabbar H. D.; AbdulRazzaq M. J.; Salim E. T.; Azzahrani A. S.; Ibrahim R. K.; Ismail R. A., Preparation of GaN/Porous silicon heterojunction photodetector by laser deposition technique, Scientific Reports, 13(1), 14746 (2023) 10.1038/s41598-023-41396-8.
[108] C. Shi, A. Rani, B. Thomson, R. Debnath, A. Motayed, D. E. Ioannou, and Q. Li, Appl. Phys. Lett., 115, 121602 (2019).
[109] Rashed, R. S., Fakhri, M. A., Alwahib, A. A., Qaeed, M. A., Gopinath, S. C. B., Physical Investigations of GaN/Porous Silicon at Different Laser Wavelengths, International Journal of Nanoelectronics and Materials, 2024, 17(Special issue), pp. 77–86.
[110] I.-P. Liu, C.-H. Chang, Y.-M. Huang, and K.-W. Lin, Int. J. Hydrogen Energy, 44, 5748 (2019).

[111] Abbas, A. R., Fakhri, M. A., Alwahib, A. A., Qaeed, M. A., Gopinath, S.C.B., Optical Properties of Gallium Nitride Heterostructures Grown on Quartz Using Pulse Laser Deposition Method, International Journal of Nanoelectronics and Materials, 2024, 17(June Special issue), pp. 175–180.

[112] I.-P. Liu, C.-H. Chang, H.-H. Lu, and K.-W. Lin, Sensors Actuators B, 296, 126599 (2019).

[113] Fakhri, Makram A., Salim, Evan T., Ketab, Marwah R., Jabbar, Haneen D., Ibrahim, Omar A., Azzahrani, Ahmad S., AbdulRazzaq, Mohammed Jalal, Ismail, Raid A., Basem, Ali, Alsultany, Forat H. Gopinath, Subash C. B., Optimizing charge transport in hybrid GaN-PEDOT:PSS/PMMADevice for advanced application, *Scientific Reports*14(1), 12841 (2024).

[114] H.-I. Chen, C.-H. Chang, H.-H. Lu, I.-P. Liu, and W.-C. Liu, Sensors Actuators B, 262, 852 (2018).

[115] Abdul Amir H. A. A.; Fakhri M. A.; A. Alwahib A.; Salim E. T.; Alsultany F. H.; Hashim U., An investigation on GaN/ porous-Si NO2 gas sensor fabricated by pulsed laser ablation in liquid, Sensors and Actuators B: Chemical, 367, 132163 (2022) 10.1016/j.snb.2022.132163.

[116] I.-P. Liu, C.-H. Chang, B.-Y. Ke, and K.-W. Lin, IEEE Sens. J., 19, 10207 (2019).

[117] Fakhri M. A.; Alwahib A. A.; Salim E. T.; Abdul Amir H. A. A.; Alsultany F. H.; Hashim U., Synthesis and characterization of GaN/quartz nanostructure using pulsed laser ablation in liquid, Physica Scripta, 97(11), 115813 (2022) 10.1088/1402-4896/ac9866.

[118] S. Jung, K. H. Baik, F. Ren, S. J. Pearton, and S. Jang, ECS J. Solid State Sci. Technol., 7, Q3020 (2018).

[119] Abdul Amir H. A. A.; Alwahib A. A.; Fakhri M. A., Some of Physical Properties of Neno GaN Ablated Using Pulsed Laser in Ethanol, AIP Conference Proceedings, 2660, 20137 (2022) 10.1063/5.0107771.

[120] J.-F. Xiao, C.-P. Hsu, I. Sarangadharan, G.-Y. Lee, J.-I. Chyi, and Y.-L. Wang, ECS J. Solid State Sci. Technol., 5, Q137 (2016).

[121] Jabbar H. D.; Fakhri M. A.; Razzaq M. J. A.; Dahham O. S.; Salim E. T.; Alsultany F. H.; Hashim U. Effect of Different Etching Time on Fabrication of an Optoelectronic Device Based on GaN/Psi, Journal of Renewable Materials, 11(3), 1101-1122 (2023) 10.32604/jrm.2023.023698.

[122] S. Jung, K. H. Baik, F. Ren, S. J. Pearton, and S. Jang, J. Electrochem. Soc., 164, B417 (2017).

[123] Fakhri M. A.; Alwahib A. A.; Salim E. T.; Ismail R. A.; Amir H. A. A. A.; Ibrahim R. K.; Alhasan S. F. H.; Alsultany F. H.; Salim Z. T.; Gopinath S. C. B., Preparation and Characterization of UV-Enhanced GaN/ Porous Si Photodetector using PLA in Liquid, Silicon, 15(17), 7523-7540 (2023) 10.1007/s12633-023-02528-x.

[124] M. Miyoshi, S. Fujita, and T. Egawa, J. Vac. Sci. Technol. B, 33, 013001 (2015).

[125] Fakhri, Makram A, Alwahib, Ali Abdulkhaleq, Ibrahim, Raed Khalid, Salim, Evan T., Abbas, Abeer R., Alsultany, Forat H., Gopinath, Subash C. B., Qaeed, Motahher A., Effect of different laser wavelengths on the optical properties of GaN/PSi and Al_2O_3/PSi thin films using the pulse laser deposition method, Journal of Optics (India), 2025, 475402, 10.1007/s12596-024-02393-w.

[126] R. Sokolovskij, J. Zhang, E. Iervolino, C. Zhao, and G. Q. Zhang, Sensors Actuators B, 274, 636 (2018).

[127] Abeer R Abbas, Makram A Fakhri, Ali Abdulkhaleq Alwahib, Evan T Salim, Ali B M Ali, Ahmad S Azzahrani and Subash C B Gopinath, Synthesized aluminum gallium nitride/porous-Si thin films at different compositions by pulsed laser deposition method, Physica Scripta, 2025, 100(1), 015502, 10.1088/1402-4896/ad92c5.

[128] J. Zhang, R. Sokolovskij, G. Chen, Y. Zhu, and H. Yu, Sensors Actuators B, 280, 138 (2019).

[129] Salim E. T.; Halboos H. T., Synthesis and physical properties of Ag doped niobium pentoxide thin films for Ag-Nb2O5/Si heterojunction device, Materials Research Express, 6(6), 66401 (2019) 10.1088/2053-1591/ab07d3.

[130] G. H. Chung, T. A. Vuong, and H. Kim, Results in Physics, 12, 83 (2019).

[131] Alsultany F. H.; Alhasan S. F. H.; Salim E. T., Seed Layer-Assisted Chemical Bath Deposition of Cu2O Nanoparticles on ITO-Coated Glass Substrates with Tunable Morphology, Crystallinity, and Optical Properties, Journal of Inorganic and Organometallic Polymers and Materials, 31(9), 3749-3759 (2021) 10.1007/s10904-021-02016-y.

[132] Doaa A. Mahmoud, Evan T. Salim, Rana O. Mahdi, A. Mindil, Subash C. B. Gopinath & Motahher A. Qaeed, Laser Ablation of Tungsten Metal for Au@WO3 Core-Shell Formation: A Characterizing Study at Different Laser Fluences, Plasmonics (2024). https://doi.org/10.1007/s11468-024-02607-8.

[133] Ismail R. A.; Salim E. T.; Halbos H.T., Preparation of Nb2O5 nanoflakes by hydrothermal route for photodetection applications: The role of deposition time, Optik, 245, 167778 (2021) 10.1016/j.ijleo.2021.167778.

[134] Alwazny M. S.; Ismail R. A.; Salim E. T., Aggregation threshold for Novel Au – LiNbO3 core/shell Nano composite: effect of laser ablation energy fluence, International Journal of Nanoelectronics and Materials, 15(3), 223-232 (2022).